

## Clustering in the 2dF QSO Redshift Survey

S.M. Croom<sup>1</sup>, B.J. Boyle<sup>1</sup>, N.S. Loaring<sup>2</sup>, L. Miller<sup>2</sup>, P. Outram<sup>3</sup>, T. Shanks<sup>3</sup>, R.J. Smith<sup>4</sup>, F. Hoyle<sup>5</sup>

<sup>1</sup>*Anglo-Australian Observatory, PO Box 296, Epping, NSW 2121, Australia*

<sup>2</sup>*Department of Physics, Oxford University, Keble Road, Oxford, OX1 3RH, UK.*

<sup>3</sup>*Physics Department, University of Durham, South Road, Durham, DH1 3LE, UK.*

<sup>4</sup>*Liverpool John Moores University, Twelve Quays House, Egerton Wharf, Birkenhead, CH41 1LD, UK*

<sup>5</sup>*Department of Physics, Drexel University, 3141 Chestnut Street, Philadelphia, PA 19104, USA*

**Abstract.** We present clustering results from the 2dF QSO Redshift Survey (2QZ) which currently contains over 20,000 QSOs at  $z < 3$ . The two-point correlation function of QSOs averaged over the entire survey ( $\bar{z} \simeq 1.5$ ) is found to be similar to that of local galaxies. When sub-dividing the sample as a function of redshift, we find that for an Einstein-de Sitter universe QSO clustering is constant (in comoving coordinates) over the entire redshift range probed by the 2QZ, while in a universe with  $\Omega_0 = 0.3$  and  $\lambda_0 = 0.7$  there is a marginal increase in clustering with redshift. Sub-dividing the 2QZ on the basis of apparent magnitude we find only a slight difference between the clustering of QSOs of different apparent brightness, with the brightest QSOs having marginally stronger clustering. We have made a first measurement of the redshift space distortion of QSO clustering, with the goal of determining the value of cosmological parameters (in particular  $\lambda_0$ ) from geometric distortions. The current data do not allow us to discriminate between models, however, in combination with constraints from the evolution of mass clustering we find  $\Omega_m = 1 - \lambda_0 = 0.23_{-0.13}^{+0.44}$  and  $\beta(z \sim 1.4) = 0.39_{-0.17}^{+0.18}$ . The full 2QZ data set will provide further cosmological constraints.

## 1 Introduction

The 2dF QSO Redshift Survey (2QZ) aims to compile a homogeneous catalogue of  $\sim 25000$  QSOs using the Anglo-Australian Telescope (AAT) 2-degree Field facility (2dF) [13]. This catalogue will constitute a factor of  $\gtrsim 50$  increase in numbers to a equivalent flux limit over previous data sets [5]. The main science goal of the 2QZ is to use QSOs as a probe of large-scale structure in the Universe over a range of scales from 1 to  $1000 h^{-1}$  Mpc, out to  $z \simeq 3$ . These measurements have the potential to help determine the fundamental cosmological parameters governing the Universe. The 2QZ will also significantly advance our understanding of the AGN/QSO phenomenon, by allowing us to carry out statistical studies of large numbers of QSO spectra, and also discovering rare and extreme types of AGN, for example broad-absorption-line QSOs or post-starburst QSOs [7]. As well as QSOs, there are a large number of other interesting sources being discovered including compact narrow-emission-line galaxies, white dwarfs and cataclysmic variables.

In this paper we will concentrate on the statistical measurements of QSO clustering. The basic properties of the 2QZ are outlined in Section 2. We then discuss various measurements of large-scale structure including the correlation function (Section 3) and redshift-space distortions (Section 4).

## 2 The 2dF QSO Redshift Survey

The 2QZ currently (September 2001) contains 20573 QSOs below a redshift of  $z \simeq 3$ . Observations will be completed in January 2002, by which time close to 25000 QSOs will have been observed. A large fraction of the data is already publicly available; the 2QZ “10k catalogue” [11] contains spectra

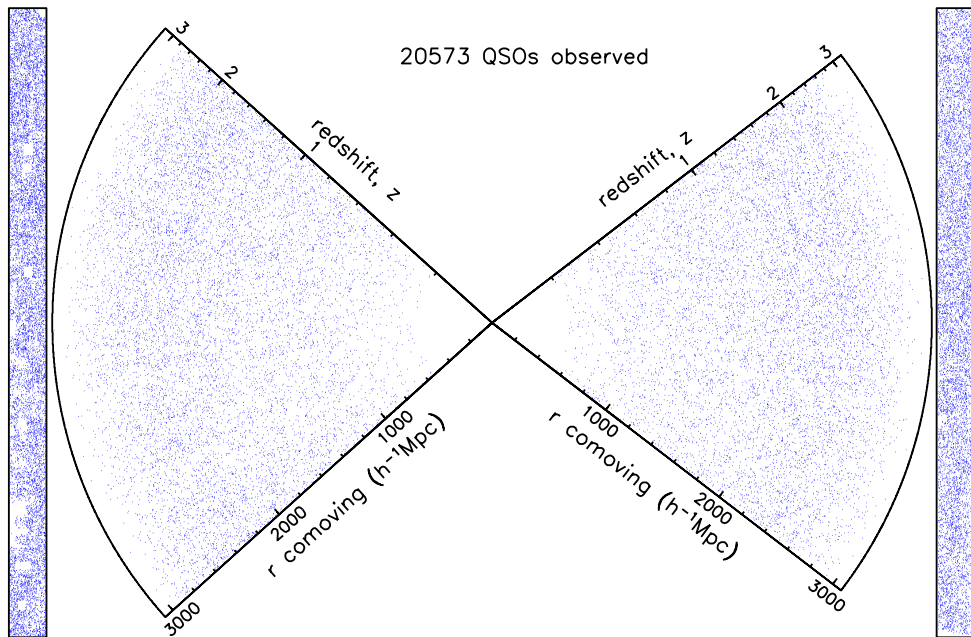


Figure 1: The spatial distribution of 2QZ QSOs as of September 2001. the SGC strip is on the left, the NGC strip on the right. The rectangles at either end show the distribution of QSOs on the sky. An Einstein-de Sitter cosmology is assumed.

of 11000 QSOs, and almost 10000 other sources. The spectra and catalogue are available electronically at <http://www.2dfquasar.org>. The analysis below mostly concerns this 10k catalogue.

QSO candidates were selected as being point sources and bluer than the stellar locus, based on broad band  $ub_Jr$  magnitudes from Automatic Plate Measuring (APM) facility measurements of UK Schmidt Telescope (UKST) photographic plates. The magnitude limits are  $18.25 < b_J \leq 20.85$ . The survey comprises 30 UKST fields, arranged in two  $75^\circ \times 5^\circ$  declination strips centred in the South Galactic Cap (SGC) at  $\delta = -30^\circ$  and the North Galactic Cap (NGC) at  $\delta = 0^\circ$  with RA ranges  $\alpha = 21^h 40$  to  $3^h 15$  and  $\alpha = 9^h 50$  to  $14^h 50$  respectively. The completed survey will cover approximately  $740 \text{ deg}^2$  [9, 17, 18].

Spectroscopic observations have been carried out using the 2dF instrument at the AAT in conjunction with the 2dF Galaxy Redshift Survey (2dFGRS) [8], as the 2QZ and 2dFGRS areas cover the same regions of sky. Spectroscopic data are reduced using the 2dF pipeline reduction system [3]. The identification of QSO spectra and redshift estimation was carried out using the AUTOZ code written specifically for this project. This program compares template spectra of QSOs, stars and galaxies to the observed spectra. Identifications are then confirmed by eye for all spectra. The mean spectroscopic completeness for the sample is 89 per cent.

The spatial and redshift distribution of QSOs is shown in Fig 1. At redshifts  $z \gtrsim 2$  the decline in QSO numbers is due to the increased reddening of QSO colours by absorption in the Ly $\alpha$  forest. QSOs in this region are therefore missed by our colour selection. At low redshifts we will miss objects in which the host galaxy contributes significantly to the flux, due to both the extended nature of the sources and their redder colours. An estimate of the survey incompleteness due to the colour selection is given by Boyle et al. (2000) [6].

### 3 The QSO correlation function

We have measured the redshift space correlation function,  $\xi_Q(s)$ , of 2QZ QSOs, both averaged over the entire sample, and sub-divided into redshift or magnitude intervals.  $\xi_Q(s)$  has been estimated assuming two representative cosmological models; the  $\Omega_0 = 1$  Einstein-de Sitter model (EdS) and a model with  $\Omega_0 = 0.3$  and  $\lambda_0 = 0.7$  ( $\Lambda$ ). We use the minimum variance [12] correlation function estimator, and details of our method can be found in Croom et al. (2001) [10].

In Fig. 2a shows the QSO correlation function for EdS and  $\Lambda$  universes averaged over  $0.3 < z \leq 2.9$ ,

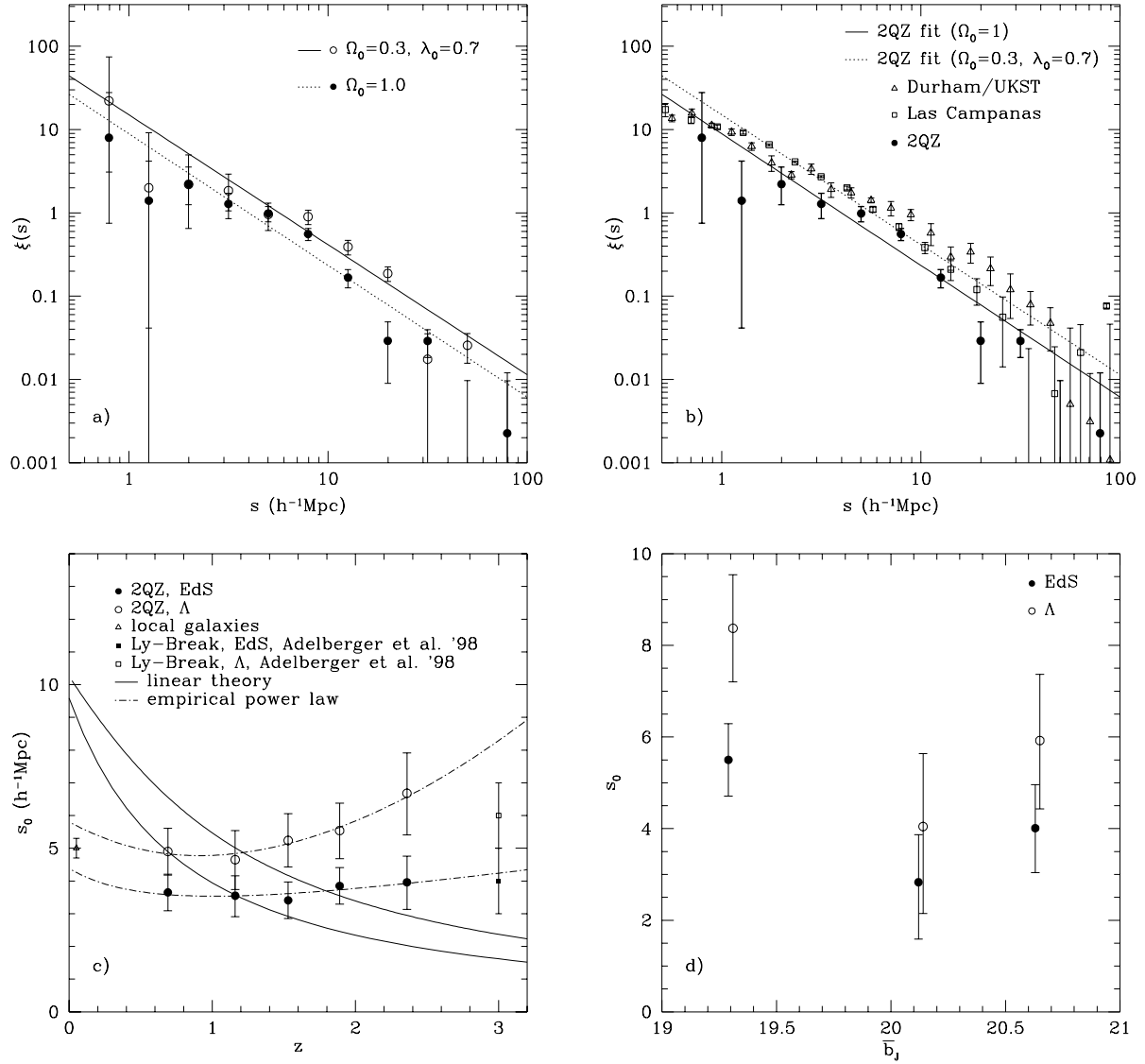


Figure 2: QSO clustering results. a) The two-point correlation function for 2QZ QSOs in the redshift interval  $0.3 < z \leq 2.9$  in EdS and  $\Lambda$  cosmologies with the best fit power law in each case. b) A comparison with the clustering of local galaxies [16,19]. The 2QZ data points for the  $\Lambda$  model are omitted for clarity. c) The values of  $s_0$  as a function of  $z$  for EdS and  $\Lambda$  cosmologies. We show the linear theory predictions (solid lines; top:  $\Lambda$ ) and the best fit empirical models (dot-dashed line). d) Clustering strength as a function of mean apparent magnitude.

based on the QSOs in the 10k catalogue. The amplitude and shape of  $\xi_Q(s)$  is comparable to that of local galaxies (Fig. 2b). Fitting a standard power law of the form  $\xi_Q(s) = (s/s_0)^{-\gamma}$  we find that  $s_0 = 3.99^{+0.28}_{-0.34} h^{-1} \text{Mpc}$  and  $\gamma = 1.55^{+0.10}_{-0.09}$  for an EdS cosmology. The effect of a significant cosmological constant is to increase the separation of QSOs, so that in the  $\Lambda$  model the best fit is  $s_0 = 5.69^{+0.42}_{-0.50} h^{-1} \text{Mpc}$  and  $\gamma = 1.56^{+0.10}_{-0.09}$ . Both these best fit lines are shown in Fig 2a.

We then sub-divide the 2QZ into five redshift intervals containing approximately equal number of QSOs. The correlation function is measured in each redshift interval separately, and a power law is fit to the result (assuming the same slope as found from the full sample). The resulting clustering scale lengths are shown in Fig. 2c. The clustering of QSOs is constant as a function of redshift over the entire range probed by the 2QZ (EdS). In the  $\Lambda$  case there is a marginal increase of clustering with increasing redshift, but a constant value cannot be ruled out. Making comparisons to the clustering of high redshift Ly-break galaxies [1], at  $z \sim 3$ , we see that these also have a similar clustering strength to that of the 2QZ QSOs. The solid lines in Fig. 2c denote the linear theory evolution of clustering. The data disagrees with the linear theory prediction, implying that QSOs must have a redshift dependent bias factor,  $b_Q(z)$ . We derive an empirical fit to the bias of the QSOs assuming

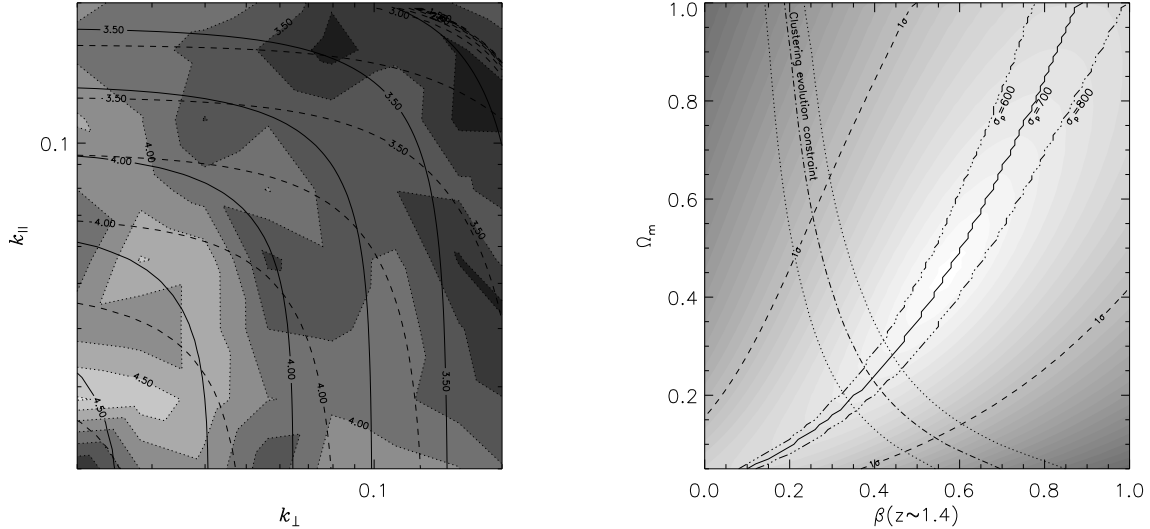


Figure 3: Left:  $P(k_{\parallel}, k_{\perp})$  estimated from the 2QZ 10k catalogue. Filled contours of constant  $\log(P(k)/h^{-3} \text{ Mpc}^3)$  are shown as a function of  $k_{\parallel}/h^{-1} \text{ Mpc}$  and  $k_{\perp}/h^{-1} \text{ Mpc}$ . Overlaid are the best fit model (solid contours) with  $\beta = 0.39$  and  $\Omega_m = 0.23$ , and a model with  $\Omega_m = 1.0$  and  $\beta = 0.19$  (dashed contours). Right: filled contours of increasing  $\chi^2$  in the  $\Omega_m - \beta$  plane for fits to the 2QZ 10k catalogue. The solid line represents the best fit value of  $\beta$  for each  $\Omega_m$  and the  $1-\sigma$  statistical error is given by the dashed line. The dot-dot-dot-dash lines above and below the solid line show the best fit value of  $\beta$  for each  $\Omega_m$  with  $\sigma_p = 600 \text{ km s}^{-1}$  and  $\sigma_p = 800 \text{ km s}^{-1}$  respectively. Overlaid is the best-fit (dot-dash) and  $1-\sigma$  (dot) values of  $\beta$  determined using the mass clustering evolution method. The joint best fit values obtained are  $\beta = 0.39$  and  $\Omega_m = 0.23$ .

$b(z) = 1 + (b(0) - 1)G(\Omega_0, \lambda_0, z)^\beta$  where  $G(\Omega_0, \lambda_0, z)$  is the linear growth factor (dot-dashed lines in Fig. 2c). The best fit values are  $b(0) = 1.45_{-0.16}^{+0.21}$  and  $\beta = 1.68_{-0.40}^{+0.44}$  (EdS) and  $b(0) = 1.28_{-0.11}^{+0.16}$  and  $\beta = 1.89_{-0.46}^{+0.49}$  ( $\Lambda$ ). A more detailed analysis is carried out by Croom et al. (2001) [10].

We lastly sub-divide our sample into 3 apparent magnitude slices with equal number of QSOs in each. The measured values of  $s_0$  as a function of mean apparent magnitude are shown in Fig. 2d. There is no significant difference between the different magnitude slices, although the brightest QSOs do have marginally stronger clustering. We note that sub-dividing on the basis of apparent magnitude is approximately equivalent to selection relative to  $M^*$  due to the extreme luminosity evolution of QSOs over the redshift range of our sample [6].

#### 4 Cosmological parameters from redshift-space distortions

By comparing clustering along and across the line of sight, and modelling the effects of peculiar velocities (both linear and non-linear) it is possible to detect the geometric distortions present if the wrong cosmological model is assumed when determining the clustering [2, 4]. At high redshift, the geometric distortion is particularly sensitive to the cosmological constant  $\lambda_0$ . In practice, a model which also takes into account linear infall is fit to provide a constraint in the  $\lambda_0$  vs.  $\beta = \Omega_0^{0.6}/b$  plane.

The QSO power spectrum from the 2QZ 10k sample, measured along and across the line of sight,  $P(k_{\parallel}, k_{\perp})$ , is shown in Fig. 3. Unfortunately the current 2QZ data only provides a joint constraint on  $\Omega_m = 1 - \lambda_0$  and  $\beta$  (shading in Fig. 3b). In fact there is also some dependence on the value of the small scale non-linear pair-wise velocity dispersion,  $\sigma_p$ . Because we are looking at  $P(k_{\parallel}, k_{\perp})$  on large scales this is not a major issue, but the effects of varying the assumed velocity dispersion is shown in Fig. 3b.

However, we can obtain a useful constraint on the cosmological world model by combining the above approach with our knowledge of the linear growth of clustering. By using the value of  $\beta$  and the two-point correlation function for nearby galaxies derived from the 2dfGRS [15] we can determine the

clustering of matter at  $z = 0$  and for a given cosmology we can then derive the clustering of mass as a function of  $z$ . Comparison to the amplitude of QSO clustering then gives the mean value of the QSO bias and hence  $\beta$ . This approach gives a differing relation between  $\Omega_m$  and  $\beta$  (dotted and dot-dashed lines in Fig. 3b), and thus breaks the degeneracy. The current best fit derived from this method is  $\Omega_m = 0.23_{-0.13}^{+0.44}$  and  $\beta = 0.39_{-0.17}^{+0.18}$ . This analysis is discussed further in Outram et al., (2001) [14].

With the completion of the 2QZ at the end of 2001, analysis of the complete data set will produce further constraints on cosmological world models. This will include different types of analysis than those discussed here, including the gravitational lensing properties of the 2QZ QSOs. It is hoped that the 2QZ will become a major resource for the astronomical community, particularly when the final data becomes public at the end of 2002.

**Acknowledgements.** We warmly thank all the present and former staff of the Anglo-Australian Observatory for their work in building and operating the 2dF facility. The 2QZ is based on observations made with the Anglo-Australian Telescope and the UK Schmidt Telescope. NSL is supported by a PPARC Studentship. We also thank Marie and Laurence for organising a very enjoyable and interesting meeting.

## References

- [1] Adelberger K. L., Steidel C. C., Giavalisco M., Dickinson M., Pettini M., Kellogg M., 1998, *ApJ*, 505, 18
- [2] Alcock C., Paczyński B., 1979, *Nature*, 281, 358
- [3] Bailey J., Glazebrook K., 1999, 2dF User Manual, Anglo-Australian Observatory
- [4] Ballinger W. E., Peacock J. A., Heavens A. F., 1996, *MNRAS*, 282, 877
- [5] Boyle B. J., Fong R., Shanks T., Peterson B. A., 1990, *MNRAS* 243, 1
- [6] Boyle B. J., Shanks T., Croom S. M., Smith R. J., Miller L., Loaring N., Heymans C., 2000, *MNRAS*, 317, 1014
- [7] Brotherton M. S. et al., 1999, *ApJ*, 520, L87
- [8] Colless M., 1999, in Morganti R., Couch W. J., eds., *Proc. ESO/Australia Workshop, Looking Deep in the Southern Sky*. Springer-Verlag, p.9
- [9] Croom S. M., 1997, Ph.D. Thesis, University of Durham
- [10] Croom S. M., Shanks T., Boyle B. J., Smith R. J., Miller L., Loaring N., Hoyle F., 2001, *MNRAS*, 325, 483
- [11] Croom S. M., Smith R. J., Boyle B. J., Shanks T., Loaring N. S., Miller L., Lewis I. J., 2001, *MNRAS*, 322, L29
- [12] Landy, S. D., Szalay, A. S., 1993, *ApJ*, 412, 64
- [13] Lewis I. J. et al., 2001, *MNRAS* submitted
- [14] Outram P. J., Hoyle F., Shanks T., Boyle B. J., Croom S. M., Loaring N. S., Miller L., Smith R. J., 2001, *MNRAS*, in press, (astro-ph/0106012)
- [15] Peacock, J. A. et al., 2001, *Nature*, 410, 169
- [16] Ratcliffe A., Shanks T., Parker Q. A., Fong R., 1998, *MNRAS*, 296, 173
- [17] Smith R. J., 1998, Ph.D. Thesis, University of Cambridge
- [18] Smith R. J., Croom S. M., Boyle B. J., Shanks T., Miller L., Loaring N. S., 2001, *MNRAS*, submitted
- [19] Tucker D. L. et al., 1997, *MNRAS*, 285, L5